ONERA Research Icing Wind Tunnel

Pierre Berthoumieu, Baptiste Déjean, Virginel Bodoc, Thomas Alary

ONERA Research Icing Wind Tunnel

Pierre Berthoumieu[1], Baptiste Déjean[2], Virginel Bodoc [3], Thomas Alary[4]
ONERA 2 Avenue Edouard Belin 31055 TOULOUSE France

Abstract

The ONERA Research Icing Wind Tunnel was built in order to investigate SLD behavior. It was designed for 300 µm drops and to simulate realistic conditions in terms of pressure and temperature and close in velocity. Several studies have been already conduct concerning SLD impact, ice accretion and characterization. This ice wind tunnel has highlighted a good capacity to adapt to several conditions and studies and is easy to use and fast to reach conditions.

I.Introduction

For many years, ONERA is involved in icing-related activities, which gave rise to calculation tools used by manufacturers in the aerospace sector (IGLOO2D and IGLOO3D). The current evolution of the regulations requires an adaptation of simulation tools to take into account icing conditions currently untreated. This improved knowledge of the phenomena and, in consequence, development of CFD tools, can only be obtained from basic experiments using appropriate investigation means.

The new regulation needs a better knowledge of SLD Icing conditions (EASA, 2016). The PHYSICE project, funded by the DGAC has allowed ONERA to progress on large droplets impact (Berthoumieu & Déjean, 2017) (Bodoc, Berthoumieu, & Trontin, 2019) but a new step must be taken forward in working in icing conditions. ONERA had used in the past its large wind tunnel S1 in Modane Avrieux to proceed tests under icing conditions in winter, when outside temperature was low enough. Considering the evolution of the requirements, ONERA started the construction of a new research icing wind tunnel mainly dedicated to SLD.

The purpose of this tunnel is to provide a high velocity cold airflow charged with large water droplets to simulate the operating conditions of an aircraft in flight. This wind tunnel runs in a closed loop in order to regulate the temperature of the flow with a minimal energy consumption while ensuring a straight path of the water droplets.

The tunnel allows variations in air velocity, temperature and pressure as well as drop size. The following assumptions were made for dimensioning purpose:

- Rectangular test section 100 x 200 mm and 500 mm length
- Air velocity in the duct: 50 to 150 m/s
- Air temperature: -40 ° C to 30 ° C
- The velocity and temperature of the drops must be as close as possible to the carrier airflow in the test section
- Relative humidity initially controlled.
- Liquid water content up to 10 g / m3.
- In order to simulate altitude effects the facility need to run in vacuum conditions (down to 0.2 bars in absolute pressure)

All these criteria have shown the need for a vertical wind tunnel. After simulations, it was found that a horizontal configuration of the wind tunnel do not allows rectilinear trajectories for large drops due to the effect of gravity, which is not negligible regarding the sizes of drops.

The last constrain was the wind tunnel location, it should be installed in an existing building which has a room open on three levels.

[1] Research engineer, DMPE,
[2] Research engineer, DMPE,
[3] Research engineer, DMPE,
[4] PhD Student, DMPE,

II.Wind tunnel design

This chapter describes each element of the wind tunnel. They are visible on the 3D drawing presented in Figure 1, each one with its label corresponding to the description paragraph.

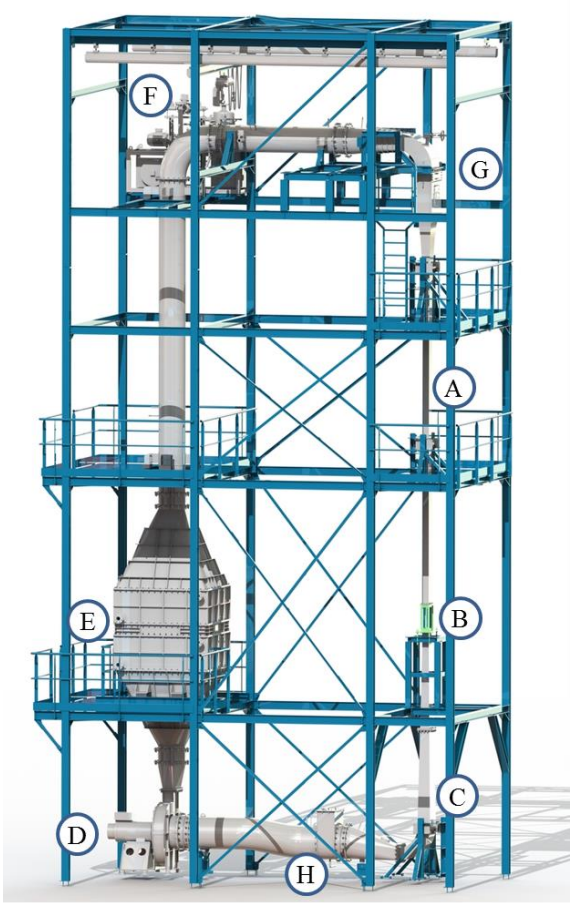

Figure 1: 3D win tunnel sketch

A. The convergent

The first element to be designed was the convergent. Its geometry was optimized for 300 microns drops in a 150 m/s air flow at the test section. The objective was to accelerate such a droplet without breakup. A specific tool was developed in order to test various geometries. It is based on classical particle motion equations coupled with a Weber number calculation. In the literature on the secondary fragmentation of drops by aerodynamic effects, the Weber number is used to define the limit below which a drop maintains its cohesion.

$$We = \frac{\rho_{air}(U_{air} - U_{drop})^2 d_{drop}}{\sigma}$$

This value varies between 10 and 12 according to different authors, beyond this value the breakup of the drop occurs.

The objective is to accelerate drops from the injection velocity (few meters per second) to the highest possible speed (the target value was set to 150 m/s).

Several convergent shapes were simulated in order to identify the optimal geometry. The drops characteristics are shown in Figure 2 for 300 µm drops in a cold (-30 ° C) airflow at 150 m / s in the test section and at ambient pressure.

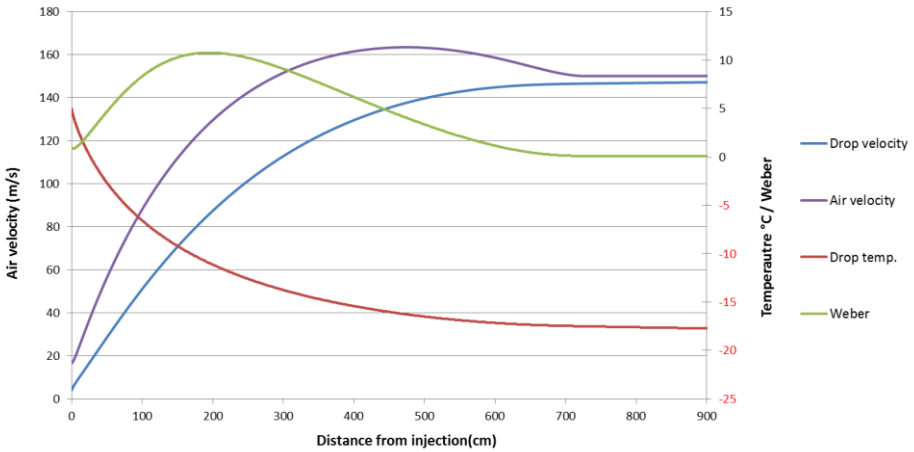

Figure 2: Droplet characteristics along the convergent (d = 300 µm, air velocity=150 m/s)

The optimal geometry assures the dynamic quasi-equilibrium after 7 m from the injection point but it is not possible to obtain the thermal equilibrium due to the limited thermal exchange between the two phases. The slip velocity between the air and the drops becomes too small to promote heat exchange. In this case, the only solution would be to increase considerably the length of the convergent, beyond the physical available place.

The keep geometry allows working with larger droplets but at a lower airflow velocity. As an example, the use of 1 mm droplet will limit the airflow velocity at 50 m/s to avoid breakup.

B. The test section

To promote the use of optical measurement system and visualization the test section is provided with 4 independent faces (Figure 2) that can be used to fix the model or be replaced by transparent windows.

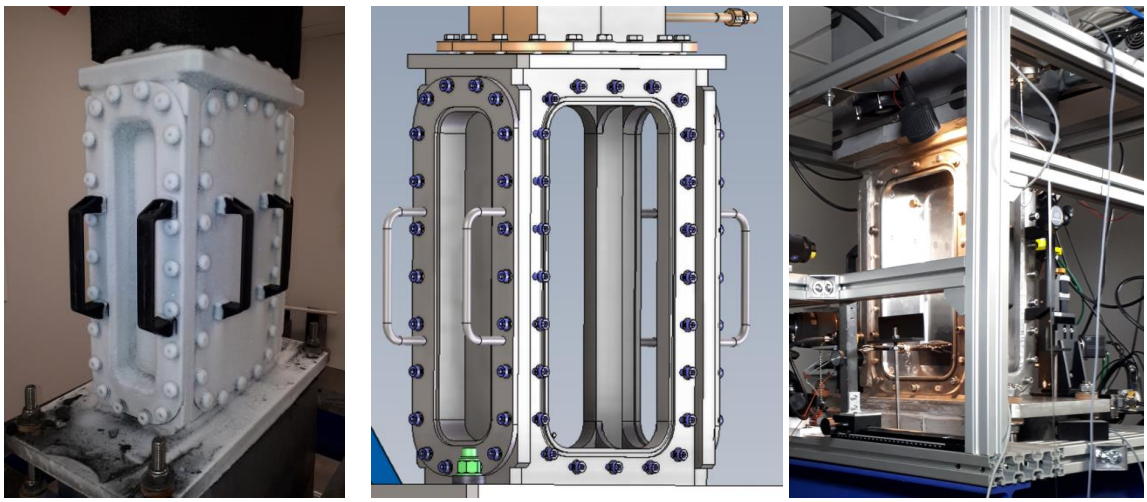

Figure 3: Test section

C. The diffuser

The diffuser is located just downstream of the test section duct. The cross sectional area of diffuser increases slowly to avoid recirculation of flow. The diffuser reduces the fluid kinetic energy while increasing the static pressure inside the duct. It decelerates the high-speed flow. The flow through a diffuser depends on its geometry defined by the diffuser angle. In this case, two angles were used 1° and 2° to increase the section by more than 5. A first evaluation of pressure drop in the whole circuit was done by using friction coefficients from the Handbook of Hydraulic Resistance from I.E. Idel'Cik (Idelchik, 1986). This kind of calculation is useful to have a first estimation of the fan power and consequently the one of the cooling unit. The final sizing of each element was iteratively obtained. When the design was well defined, a complete Navier-Stockes calculation has been made to have a more precise value of the pressure drop. A permanent flow field was calculated, the turbulence was taken into account by a standard k-epsilon model and an ideal gas was used taking into account the compressibility. The NS calculation showed that the pressure drop was higher than the estimated one. The calculation with 150 m/s in the test section at ambient pressure and -40 °C find a pressure drop of 9 000 Pa for the whole circuit. This value was maximised for the fan choice.

D. The fan

The fan (Figure 3) is sized to fight against the pressure drop of the wind tunnel circuit added of 5 000 Pa to anticipate the presence of a model in the test section and uncertainties in the simulation. This fan is fully sealed to prevent leakage during altitude simulation operations. It has been designed by Howden, various operating points were used to refine the design of the fan blades. They were chosen to sweep the entire working area of the wind tunnel. The most restrictive case corresponds to the atmospheric pressure and temperature of -40 ° C with a velocity of 150 m/s in the test section. In this case, the fan should provide a useful pressure difference higher than 14 000 Pa. For this condition the rotation velocity reach 3 110 rpm. The fan is driven by an Obeki motor of 62 kW. This motor is fully sealed and it can works without damages up to 0.2 bars. Cooling of electrical motor is provided by water circulation.

Figure 4: The fan

E. The cooling system

The next element is the cooling system (Figure 4); it is composed of two parts the chiller and the heat exchanger. The chiller used a R448A refrigerant. It provides an excellent combination of low Global Warming Potential (GWP) and high-energy efficiency. It offers reduced compressor discharge temperature at medium and low temperature conditions. The chiller has been studied and manufactured by CLAUGER, which is a French company specializing in industrial refrigeration and air-conditioning systems. The cooling system was sized so that the cooling time of the installation was limited to two hours to reach the minimum temperature of -40 ° C. It is made up of four independent compressors, each providing 25% of the total required power. This assembly allows finer regulation. This production of cold is coupled with significant storage in a 600 l reservoir of coolant carrier liquid, Therminol® D-12. A pump circulates this fluid in the two stainless steel heat exchangers, located inside the air circuit and giving an exchange surface of 600 m². In this exchanging zone, the air velocity is reduced in order to maximize the heat

exchanges. A grid is located just before the first exchanger in order to homogenize the airflow and take full advantage of exchanges.

Figure 5: Cooling unit and heat exchanger

F. Vacuum pump

The vacuum pump (Figure 5) is positioned in the upper part of the wind tunnel; it is dimensioned to maintain the assembly at a pressure of 0.2 bars independently of the use of assistance air for the injection of drops. The chosen technology is a liquid-ring pump that can extract up to 52 Kg/h of air at 0°C. With this configuration the pressure decrease in the wind tunnel takes less than 10 minutes.

Figure 6: Vacuum pump

This device will be also used to remove humid air from the wind tunnel and refill it with dry air in order to control the humidity level before each run.

A particular attention has been paid to the sealing of the duct because during vacuum tests the presence of leaks could allow the entry of ambient air with a high humidity level and thus pollute the air inside the wind tunnel.

G. Droplet injection

Droplets are injected in a settling chamber just before the convergent (Figure 6).

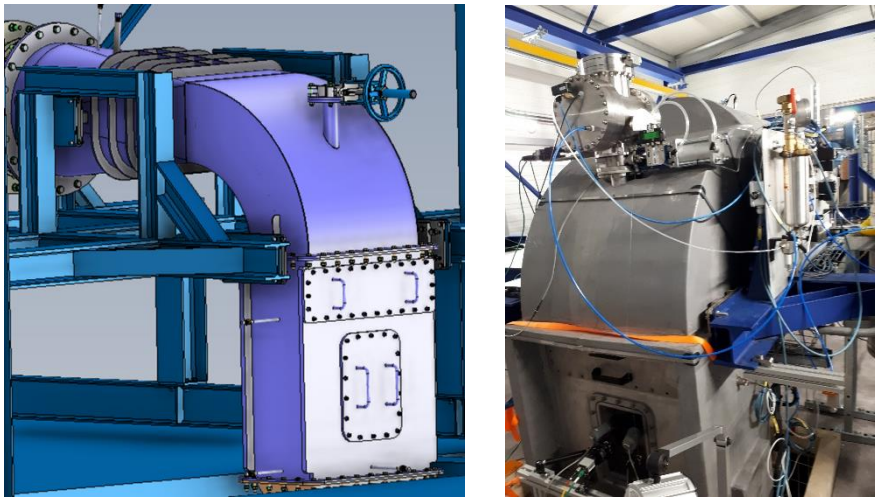

Figure 7: Droplet injection zone

Two possibilities of water injection are present:

- A classic air-assisted spray system to reproduce the usual droplet size distributions: A system from Spraying system was chosen with different combinations of air and liquid nozzles in order to be able to produce a wide range of liquid flow rates and mean drop sizes. The system is controlled by two pressure modulators. This system allows the flowrate to be varied until 15g/s with droplet MVD from 20 to 60 µm

- A monosize drop generation system, using an injector provided with an electric piezo ceramic. This solution will be used for parametric research on the influence of external conditions on the impact of the drops and their accretion. Droplets are generated by applying a mechanical excitation on a small diameter liquid jet. The excitation is given by a piezoelectric ceramic driven by a function generator. The droplet size is directly linked to the excitation frequency imposed at the ceramic, the diameter of the liquid jet which is fixed by the exit hole of the injector, and the liquid flow rate. The relationships shown below are used to determine optimal injection conditions:

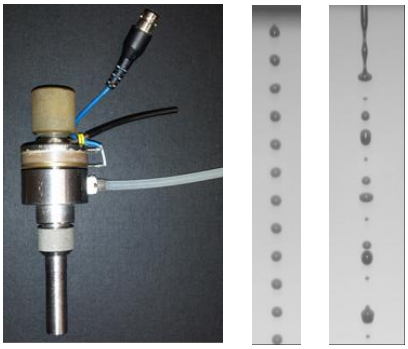

Figure 8: Droplet generator and stream
(left: injector, center: with excitation, right: without)

Droplet diameter:	$D_d = \sqrt[3]{\frac{6Q}{\pi f}}$
Droplet spacing:	$S_d = \frac{V_d}{f}$
Optimal excitation wavelength given by Rayleigh theory:	$\lambda_{opt} = 4.51\Phi_0$
Optimal frequency:	$f_{opt} = 0.198\frac{V_{inj}}{\Phi_0}$
When the optimal frequency is used, the droplet diameter is:	$D_d = 1.9\ \Phi_0$

The excitation frequency should be adapted to the liquid flow rate and the injector hole, so as to obtain a monosized droplets stream. The diameter of the drops depends essentially on the diameter of the orifice and can be slightly modified by varying the excitation frequency. The initial velocity of the drop depends essentially on the flow rate and therefore on the injection pressure. The use of this injector

makes it possible to generate drops with a speed varying between 5 and 10 m/s by modulating the injection pressure of the water. In these conditions droplet size could be managed bigger than 50 µm.

H. Drip trap

A drip trap is positioned after the test area to recover drops that have not impacted on the model or on the blades of the upstream elbow. This has to limit the accretion drops on the fan blades to not affect its performance.

To guarantee a good resistance to vacuum and corrosion the whole wind tunnel is built in 316A stainless steel. The thickness of the steel sheet is adapted to each section of the duct in order to limit the total mass of the installation. The outer insulation is made with 80 mm thickness of FOAMGLAS® in order to maintain the outer walls at a largely positive temperature.

The installation is equipped with numerous temperature and pressure sensors that are managed by a S700 SIEMENS controller. A specific supervision software has been developed, and it offers two operating modes:

- an automatic mode for which the user specifies the desired test conditions (temperature, speed and pressure condition) and the system is in charge of setting them :
- a manual mode in which the user can independently control each element of the system.

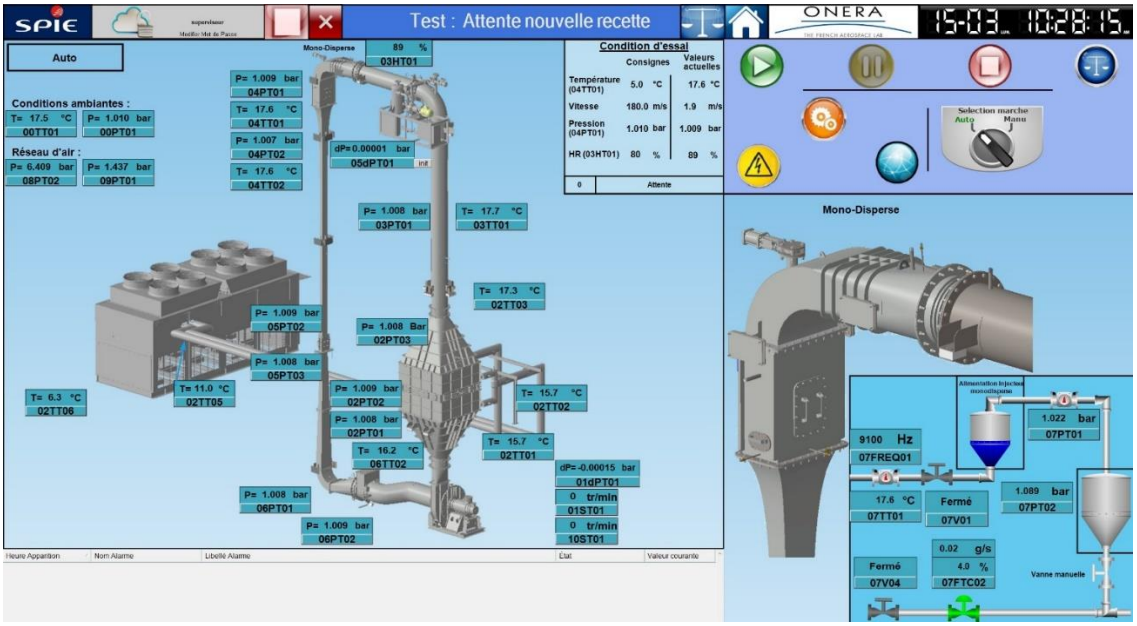

Figure 9: HMI view

III.Wind tunnel characterization

The reception of the wind tunnel started with the verification that the requested characteristics were reached. A cylindrical rod carrying out an obstruction of 10% of the test section was introduced to simulate a future model. Under these conditions, it will be possible to reach a bulk velocity of 175 m/s decreasing the static temperature down to -43°C. Several tests were conducted then and with smaller mock-ups, experiments were conducted until 190 m/s with SLD injection.

A. Airflow characterization

The characterization of the airflow (measurement of the velocity profiles) has been performed in different sections following the fourth axis defined in red, blue, orange and grey in Figure 10. The longitudinal component of the velocity has been measured with a Kiel probe positioned along each every 10 millimeters.

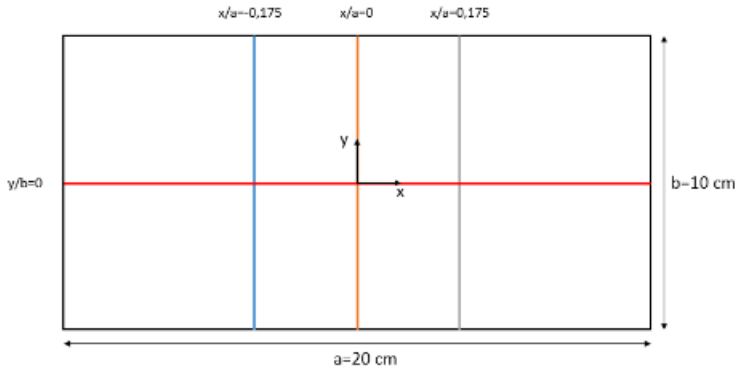

Figure 10 : ONERA Icing wind tunnel test section dimension and the positions of Kiel probe measurements. Flow direction is perpendicular to the section.

Figure 11 compares the longitudinal velocity profiles for three different maximum velocities along the transversal x-axis (y/b=0). For each profile, the velocity values are normalized by the maximal velocity. Near the wind tunnel wall, the velocity decreases as expected while in the central area of the test section, the flow velocity is almost constant over about 120 millimeters.

Figure 12 shows the same velocity profiles plotted along the y-axis median line. This shows that, along the y-axis, there is no velocity plateau neither for various distances to the symmetry plan nor for various bulk velocities.

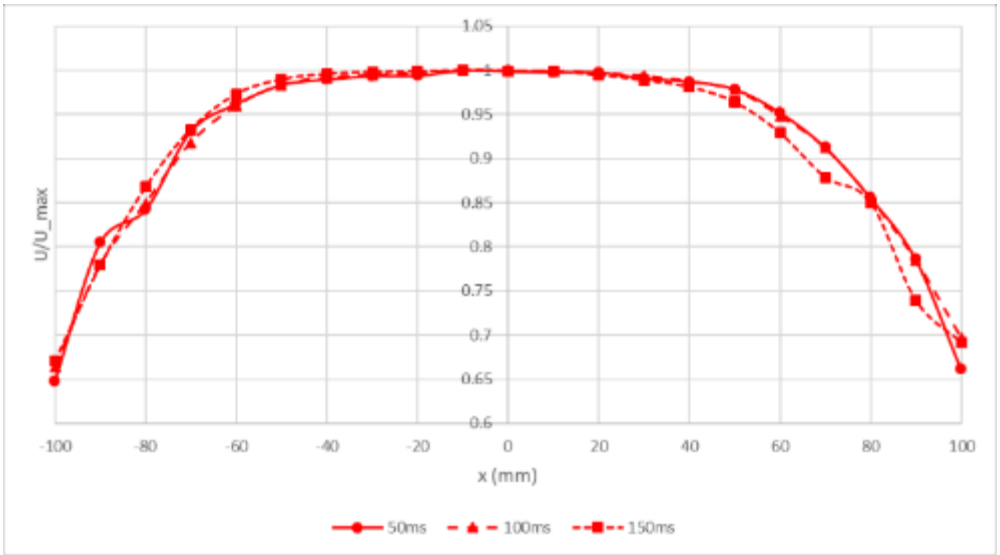

Figure 11 : Longitudinal velocity profiles (U/Umax) for 50m/s, 100m/s and 150m/s for y/b=0

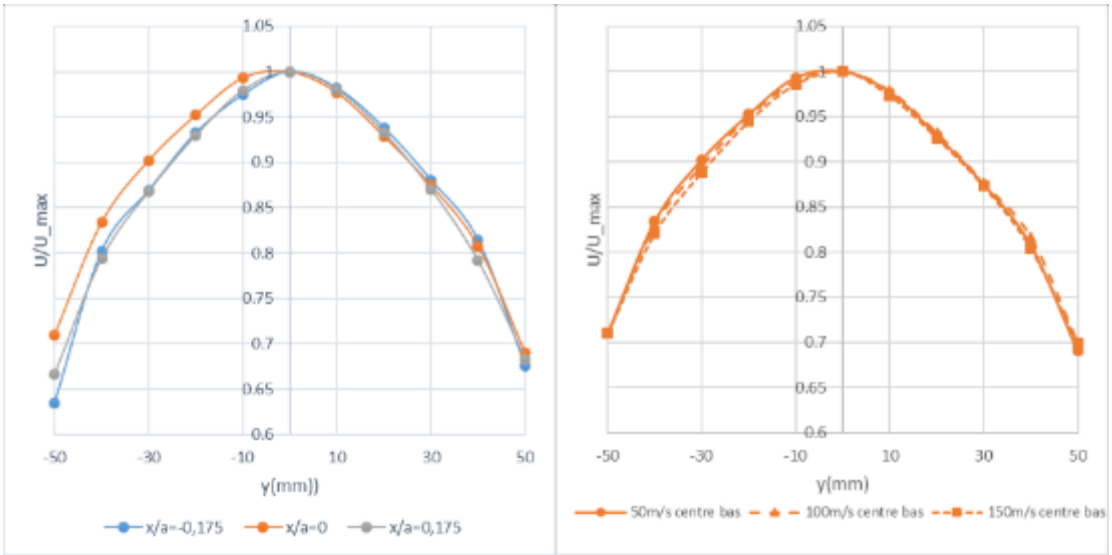

Figure 12 : Longitudinal velocity profiles along the transverse direction.
Left: various position at 50m/s, Right: 50m/s, 100m/s and 150m/s for x/a=0.

B. Drop characterization

1. Monosize injection

Droplet size and velocity

Droplet size and velocity characterisations have been carried out for different operating conditions. The measurement was performed using a camera with two flashes during aperture time (Alary, Déjean, Berthoumieu, & Trontin, 2022). The droplet size depends on the experimental conditions (droplet generator frequency, pinhole diameter, injection pressure and airflow). For each experimental condition, a droplet size histogram may be plotted as shown in Figure 13. Different discrete values are observed on this histogram and this feature is probably due to droplet coalescence inside the icing wind tunnel. For the particular result plotted on Figure 13, the first peak corresponds to the expected initial drop (175 µm), the bigger drops correspond to a mix of coalescence and then breakup of drops.

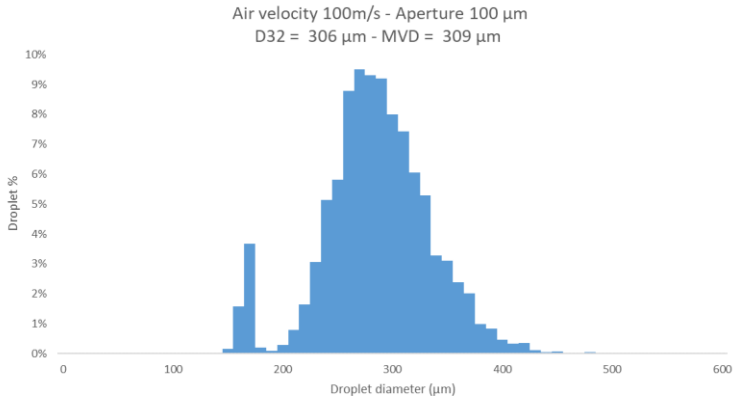

Figure 13 : Example of droplet diameter histogram
(air speed: 100m/s, pinhole: 100µm, frequency≈14kHz)

From Table 1, it may be observed that for a given pinhole diameter the mean initial droplets characteristics (size and velocity) do not vary with the air velocity. These variations are less than 3% except for the lowest airflow velocity (67 m/s). In this case, the coalescence of the drops between the injection point and the test section seems to

be more important. This behaviour may be due to the relatively low airflow velocity in the injection zone not high enough to separate the successive drops.

Droplet velocities are very close (within few percent) to these of the incoming airflow. Finally, it has also been observed that the droplets slow down as they approach the wall, entering into the stagnation zone of the obstacle.

Table 1: Mean characteristics of incoming droplets

Air velocity (m/s)	Pinhole diameter (µm)	Droplet mean diameter (µm)	D32 (µm)	MVD (µm)	Droplet mean velocity (m/s)
100	75	264	273	275	97
150	75	257	267	267	142
67	100	326	361	372	64
100	100	292	306	309	95
150	100	302	317	324	139
180	100	302	315	321	164
100	150	389	423	442	92
150	150	389	412	422	136

Droplet spatial distribution

In order to study the accretion phenomenon, it is necessary to have a description as detailed as possible of the cloud of the incoming droplets in terms of its homogeneity and local repartition. A camera and a laser sheet have been used to perform such an analysis and the optical set-up is displayed in Figure 14.

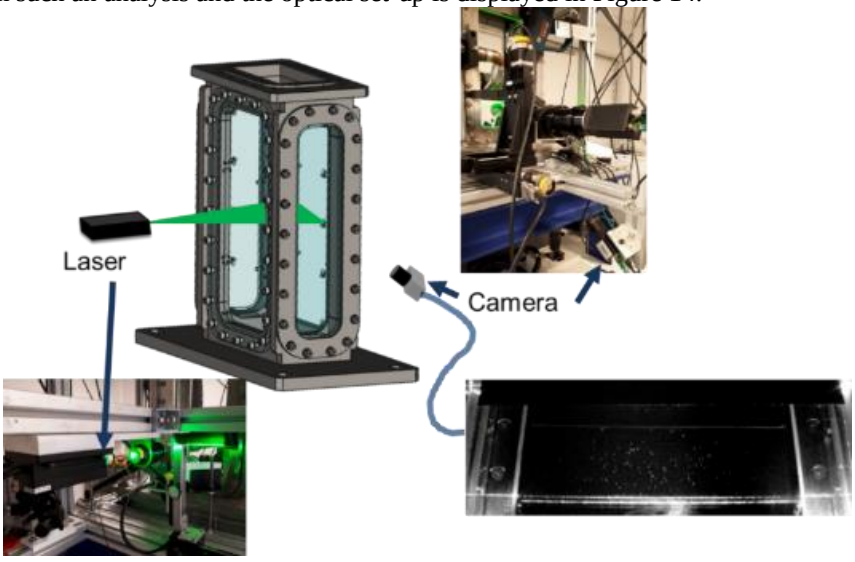

Figure 14 : Setup for the droplet spatial distribution investigation

The laser sheet illuminates the test section of the wind tunnel perpendicularly to the flow. Each drop crossing this laser sheet scatters light according to the Mie process. A camera tilted at about 45° with respect to the laser sheet takes images of these droplets. The laser sheet is located a few centimetres upstream the impingement location. Due to the linear trajectory of the droplets over such a short distance, it can be assumed that the droplet spatial distribution does not change between the measurement section and the impact location. Following the Mie scattering theory, increasing the detectability of droplets leads to place the optical receiver in the forward scattering mode since the droplet emitted light intensity is higher. This arrangement implies that the camera is viewing the scene under a tilt angle and a calibration is needed in order to dewarp the images before processing.

The camera, IDS UI 6140 SE, runs with the maximum possible exposure time in order to miss as few droplets as possible, and to obtain an accurate distribution of droplets. The exposure time is set to 19.811 milliseconds for a recording rate of 50.31 images per second. The blank time of 0.06 milliseconds between two successive images corresponds to only 0.3 % of the overall recording time. A sequence of 3 000 images is taken to characterize the droplet distribution across the section of the wind tunnel.

Once dewarped, the images are analysed, using a threshold on each image to detect the droplets and find their positions. Merging all these data provides droplet repartition cartographies such as the one presented in Figure 15. The values correspond to the number of droplets crossing the cell during the experiment.

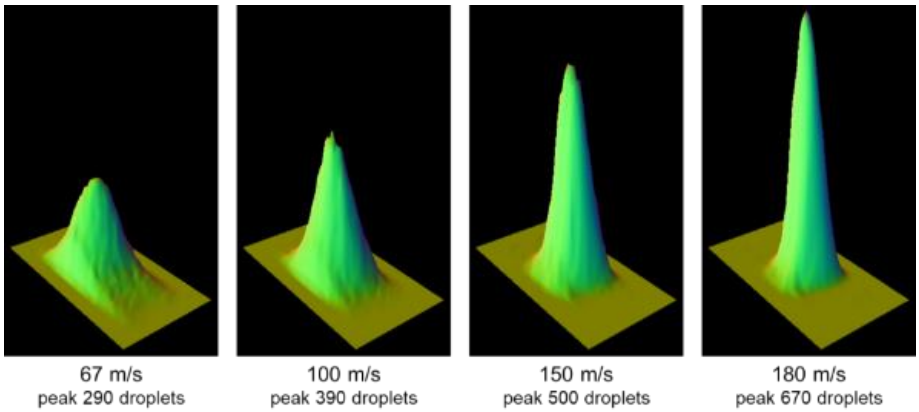

Figure 15 : Number of droplets crossing the laser sheet in one minute.

The 3D plots presented in Figure 15 represent the distribution of the number of droplets across the test channel section for different air velocity. It can be seen that the droplet dispersion is highly correlated to the air velocity, i.e., the lower the airflow velocity, the more important the droplets dispersion. In fact, when the airflow velocity increases, the droplets are subjected to more important aerodynamic forces and the cloud of droplets becomes narrower.

2. Air-assisted polydisperse system

In order to calibrate the injection system, drop size measurements by light scattering system was used outside of the wind tunnel. The measures were done at around 100 mm from the nozzle. Thus, a relationship between the value imposed to the pressure modulators and the average drop size and liquid flow rate was achieved, allowing the drop injection to be adapted to the chosen configuration.

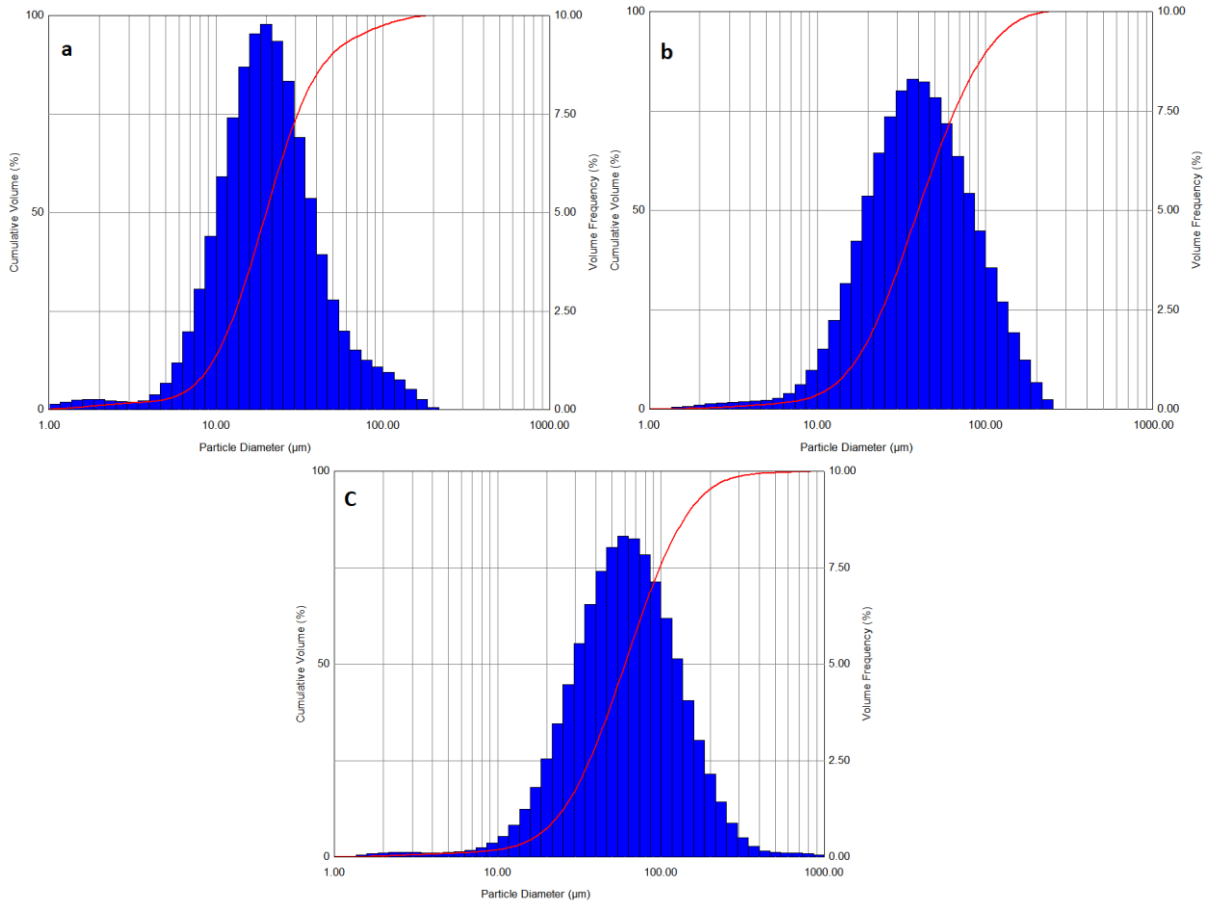

Figure 16 : examples of drop repartition for the polydisperse injector (Qm = 0.5 g/s, a: MVD = 20µm, b: MVD = 40µm, c: MVD = 60µm,)

IV.First experiments

Since the start-up of the ice wind tunnel, several studies were conducted using the different possibilities given by this installation.

- Impacts

Through the European program Ice Genesis, the impact of SLD was investigate. Visualization to describe impact and PDA measurements to characterize reemitted droplets were conducted. This experience is the subject of another paper submitted to this AIAA conference (Alary, Déjean, Berthoumieu, & Trontin, 2022).

- Accretion

In the same study, accretion in SLD condition was explored. Different behaviors were observed depending on the conditions. These results will be subjects to an article when their analysis will be finished.

- Ice samples

In collaboration to the materials and structures department of Onera (DMAS), the study of ice characteristics is lead thanks to the wind tunnel. Some realistic ice sample were generated. Their size is around 7 cm diameter and 10-12 cm high. They will be machined to obtain specimen of calibrated size in order to perform mechanical test (traction, compression).

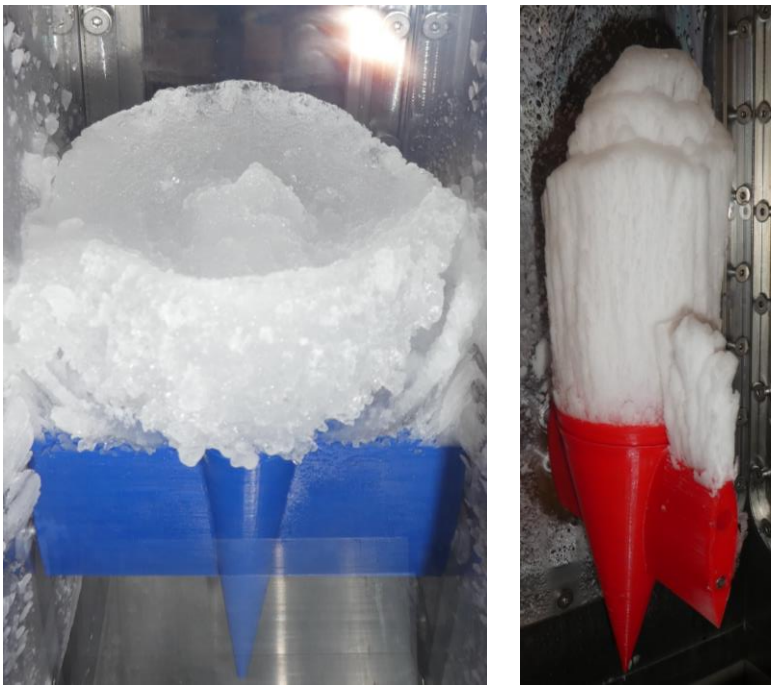

Figure 17 : sample of ice produced in realistic condition
left: glaze ice, Uair = 80m/s, T=-5.3°C, LWC=0.54, MVD = 20µm
right: rime ice, Uair = 80m/s, T=-30°C, LWC=0.54, MVD = 20µm

- Ice fracture

For the same project, some experiments are planed to investigate ice fracture. For this purpose, a dedicated mock-up was designed with a piston inserted inside (Figure 18). After a chosen accretion time, the piston is activated and break the ice layer. Thanks to high speed camera the phenomena is recorded to compare with models.

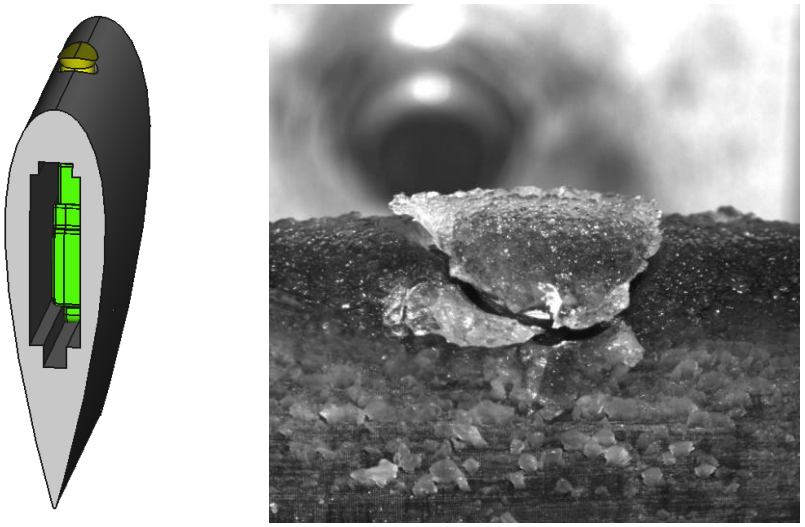

Figure 18 : left, mock-up with piston - right, example of ice fracture

V.Conclusion

This wind tunnel has unique characteristics in terms of velocity, temperature and pressure that allows ONERA to carry out new studies on the SLD impact. These studies are helping in the development of new models, which will be implemented in ONERA codes.

The first tests carried out with this installation were performed within the European project ICE GENESIS dealing with the study of the impact of SLD for different test conditions, speed, temperature and drop size. This facility is currently used for material testing to characterize ice fracture and adhesion. Several studies on the development and improvement of measurement techniques are also considered.

Acknowledgements

The authors would like to thank the DGAC – Direction Générale de l'Aviation Civile - for their participation in financing this facility.